

Novel Amphiphilic Ruthenium Sensitizer with Hydrophobic Thiophene or Thieno(3,2-*b*)thiophene-Substituted 2,2'-Dipyridylamine Ligands for Effective Nanocrystalline Dye Sensitized Solar Cells

Jeum-Jong Kim,[†] Hyunbong Choi,[†] Chulwoo Kim,[†] Moon-Sung Kang,[‡] Hong Seok Kang,[§] and Jaejung Ko^{*,†}

[†]Department of New Material Chemistry, Korea University, Jochiwon, Chungnam 339-700, Korea, [‡]Energy & Environment Laboratory, Samsung Advanced Institute of Technology (SAIT), Yongin 446-712, Korea, and [§]Department of Nano and Advanced Materials, College of Engineering, Jeonju University, Jeonju, Korea

Received July 3, 2009. Revised Manuscript Received September 16, 2009

Hydrophobic conjugated 2,2'-dipyridylamine substituted amphiphilic ruthenium complexes {*cis*-Ru(dcbpy)(L)(NCS)₂, where dcbpy is 4,4'-dicarboxylic acid-2,2'-bipyridine and L is 4,4'-di(5-hexylthiophen-2-yl)-2,2'-dipyridylamine, **JK-85**, or 4,4'-di[5-hexylthieno(3,2-*b*)thiophene]-2,2'-dipyridylamine, **JK-86**} were newly designed, synthesized, and successfully used as sensitizers for nanocrystalline dye sensitized solar cell using an electrolyte consisting of 0.6 M 1,2-dimethyl-3-propylimidazolium iodide (DMPII), 0.05 M I₂, 0.1 M LiI, and 0.5 M *tert*-butylpyridine in acetonitrile. Under standard AM 1.5 sunlight, the complex **JK-86** yielded a short-circuit photocurrent density of 18.3 mA/cm², an open-circuit voltage of 0.68 V, and a fill factor of 0.72, corresponding to an overall conversion efficiency of 9.03%. Importantly, the cell exhibits an excellent stability, revealing almost no change after 1000 h of light soaking at 60 °C using a quasi-solid-state electrolyte composed of 0.1 M I₂, 0.5 M NMBI (*n*-methylbenzimidazole), 0.6 M DMPII (1-propyl-2,3-dimethylimidazolium iodide), and 5 wt % PVDF-HFP (poly(vinylidene fluoride-*co*-hexafluoropropylene)) in MPN (3-methoxypropionitrile).

Introduction

Increasing consumption of fossil fuels causing global warming and environmental pollution dictates the development of renewable energy sources.¹ Among several new energy technologies, dye-sensitized solar cells (DSSCs) have attracted significant attention as low-cost alternatives to conventional solid photovoltaic devices.² In these cells, the sensitizer is a pivotal component for high power-conversion efficiency. Until now only four polypyridyl ruthenium sensitizers have achieved power conversion efficiencies over 11% in standard air mass 1.5 sunlight.³ To become more competitive with silicon-based photovoltaic cells, the efficiency of DSSCs needs to be improved. One of the possible approaches to increase the efficiency lies in the extension of absorption in the far-visible region as well as an increase of the optical coefficient of the sensitizer. One strategy for broadening the absorption range and increasing the molar absorption coefficient is to increase the conjugation length of

the ligand.⁴ Replacement of one of the dcbpy anchoring ligands in N3 with a highly conjugated ancillary ligand represents a molecular engineering for enhancing device efficiency.⁵ Several groups have developed an efficient ruthenium sensitizer with extended conjugation such as thiophene,⁶ thienothiophene,⁷ and alkoxybenzene moieties.⁸

*Corresponding author. Fax: 82 41 867 5396. Tel: 82 41 860 1337. E-mail: jko@korea.ac.kr.

(1) Robertson, N. *Angew. Chem., Int. Ed.* **2006**, *45*, 2338.
(2) (a) O'Ragen, B.; Grätzel, M. *Nature* **1991**, *363*, 737. (b) Grätzel, M. *Nature* **2001**, *414*, 338.
(3) (a) Nazeeruddin, M. K.; De Angelis, F.; Fantacci, S.; Selloni, A.; Viscardi, G.; Liska, P.; Ito, S.; Takeru, B.; Grätzel, M. *J. Am. Chem. Soc.* **2005**, *127*, 16835. (b) Chiba, Y.; Islam, A.; Watanabe, Y.; Komiyama, R.; Koide, N.; Han, L. *Jpn. J. Appl. Phys., Part 2* **2006**, *45*, L638. (c) Gao, F.; Wang, Y.; Shi, D.; Zhang, J.; Wang, M.; Jing, X.; Humphry-Baker, R.; Wang, P.; Zakeeruddin, S. M.; Grätzel, M. *J. Am. Chem. Soc.* **2008**, *130*, 10720. (d) Cao, Y.; Bai, Y.; Yu, Q.; Cheng, Y.; Liu, S.; Shi, D.; Gao, F.; Wang, P. *J. Phys. Chem. C* **2009**, *113*, 6290.

(4) (a) Jang, S.-R.; Lee, C.; Choi, H.; Ko, J.; Lee, J.; Vittal, R.; Kim, K.-J. *Chem. Mater.* **2006**, *18*, 5604. (b) Kim, C.; Choi, H.; Kim, S.; Baik, C.; Song, K.; Kang, M.-S.; Kang, S. O.; Ko, J. *J. Org. Chem.* **2008**, *73*, 7072. (c) Lee, C.; Yum, J.-H.; Choi, H.; Kang, S. O.; Ko, J.; Humphry-Baker, R.; Grätzel, M.; Nazeeruddin, M. K. *Inorg. Chem.* **2008**, *47*, 2267.
(5) (a) Chen, C.-Y.; Wu, S.-J.; Wu, C.-G.; Chen, J.-G.; Ho, K.-C. *Angew. Chem., Int. Ed.* **2006**, *45*, 5882. (b) Karthikeyan, C.; Wietasch, H.; Thelakkat, M. *Adv. Mater.* **2007**, *19*, 1091. (c) Chen, C.-Y.; Chen, J.-G.; Wu, S.-J.; Li, J.-Y.; Wu, C.-G.; Ho, K.-C. *Angew. Chem., Int. Ed.* **2008**, *47*, 7432. (d) O'Ragen, B. C.; Walley, K.; Juozapavicius, M.; Anderson, A.; Matar, F.; Ghaddar, T.; Zakeeruddin, S. M.; Klein, C.; Durrant, J. R. *J. Am. Chem. Soc.* **2009**, *131*, 3541.
(6) (a) Jiang, K.-J.; Masaki, N.; Xia, J.; Noda, S.; Yanagida, S. *Chem. Commun.* **2006**, 2460. (b) Chen, C.-Y.; Wu, S.-J.; Li, J.-Y.; Wu, C.-G.; Chen, J.-G.; Ho, K.-C. *Adv. Mater.* **2007**, *19*, 3888. (c) Abbotto, A.; Barolo, C.; Bellotto, L.; De Angelis, F.; Grätzel, M.; Manfredi, N.; Marini, C.; Fantacci, S.; Yum, J.-H.; Nazeeruddin, M. K. *Chem. Commun.* **2008**, 5318. (d) Shi, D.; Pootrakulchote, N.; Li, R.; Gui, J.; Wang, Y.; Zakeeruddin, S. M.; Grätzel, M.; Wang, P. *J. Phys. Chem. C* **2008**, *112*, 17046.
(7) Gao, F.; Wang, Y.; Zhang, J.; Shi, D.; Wang, M.; Humphry-Baker, R.; Wang, P.; Zakeeruddin, S. M.; Grätzel, M. *Chem. Commun.* **2008**, 2635.
(8) (a) Wang, P.; Zakeeruddin, S. M.; Moser, J.-E.; Humphry-Baker, R.; Comte, P.; Aranyos, V.; Hagfeldt, A.; Nazeeruddin, M. K.; Grätzel, M. *Adv. Mater.* **2004**, *16*, 1806. (b) Wang, P.; Klein, C.; Humphry-Baker, R.; Zakeeruddin, S. M.; Grätzel, M. *J. Am. Chem. Soc.* **2005**, *127*, 808. (c) Kuang, D.; Klein, C.; Ito, S.; Moser, J.-E.; Humphry-Baker, R.; Evans, N.; Durrant, F.; Grätzel, C.; Zakeeruddin, S. M.; Grätzel, M. *Adv. Mater.* **2007**, *19*, 1133.

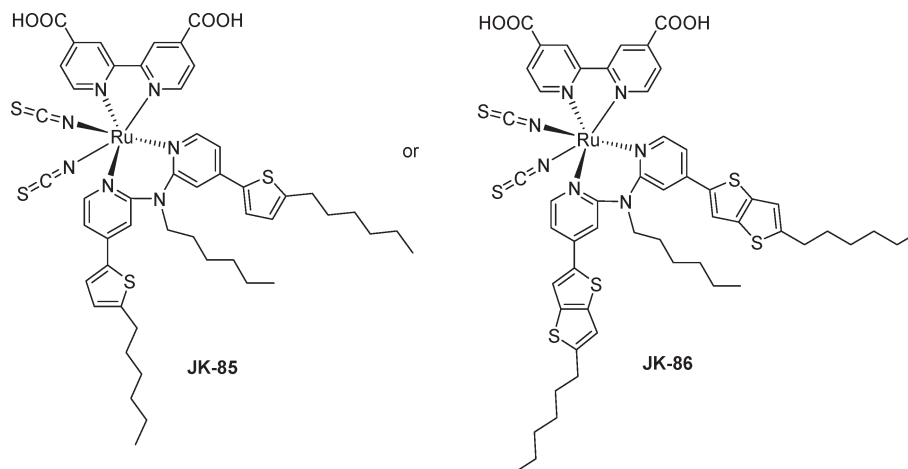


Figure 1. Molecular structures of **JK-85** and **JK-86**.

In the second approach, judicious tuning of the HOMO and LUMO levels of a dye, including lifting the HOMO level by introducing σ -donor ligand or lowering the LUMO level by incorporating π -acceptor ligands, is the specific strategy to be pursued in the molecular design of dyes.⁹ In this context, Wang et al.¹⁰ and Masuda et al.¹¹ reported amphiphilic polypyridyl ruthenium sensitizers with 2,2'-dipyridylamine derivatives (DPA-R). The alkyl-substituted dipyrindyl derivative forms a six-membered ring with less π -acceptor character on chelation than a five-membered ring for bipyridine. The HOMO level of its ruthenium dyes is lifted due to the more σ -donating power of the amine, resulting in red-shifting the metal-to-ligand charge transfer (MLCT) band. It is well established that thiophene,⁶ thienothiophene,⁷ and alkoxybenzene⁸ derived units are the good candidates for increasing the conjugation length of the ancillary ligand to increase the light-harvesting and red-shifting of the MLCT band of a ruthenium complex. Accordingly, it is interesting to extend the conjugated system of the DPA-R ligand using such units to enhance the molar extinction coefficient as well as broaden the absorption region. Here we report the synthesis of amphiphilic ruthenium(II) sensitizers incorporating highly conjugated DPA-R ligands and their photovoltaic performance in DSSCs. The molecular structure of the two ruthenium(II) complexes [Ru(dcbpy)(L)(NCS)₂], where dcbpy is bis(2,2'-bipyridyl)-4,4'-dicarboxylic acid and L is *N*-hexyl-4,4'-di(5-hexylthiophen-2-yl)-2,2'-dipyridylamine (**JK-85**) or *N*-hexyl-4,4'-di(5-hexylthieno(3,2-*b*)-thiophene)-2,2'-dipyridylamine (**JK-86**), are shown in Figure 1.

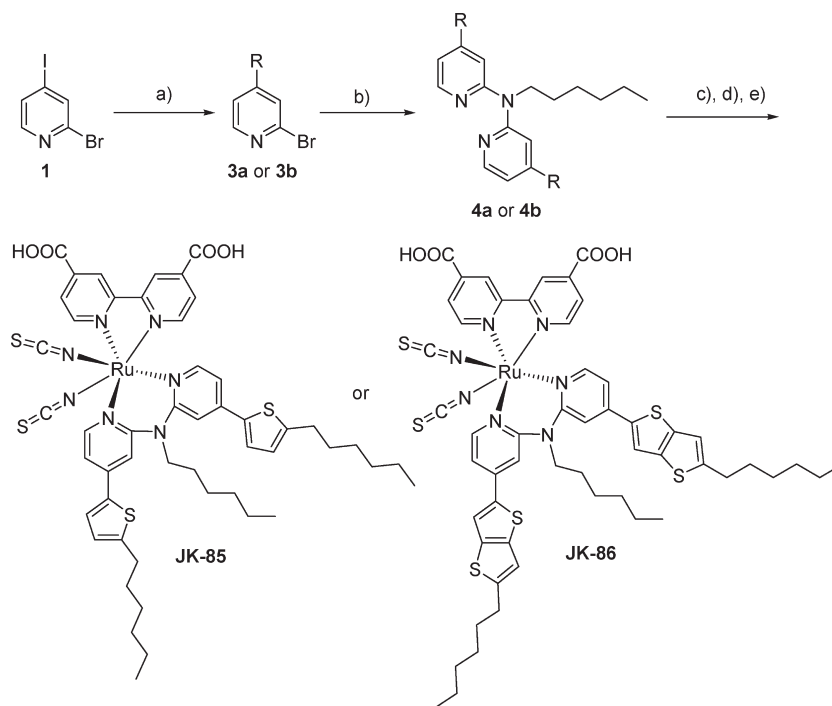
Experimental Section

All of the reactions were carried out under an argon atmosphere. ¹H and ¹³C NMR spectra were recorded on a Varian Mercury 300 spectrometer. UV-vis spectra were recorded in a 1 cm path length quartz cell on a Cary 5 spectrophotometer.

- (9) Anderson, P. A.; Strouse, G. F.; Treadway, T. A.; Keene, F. R.; Meyer, T. J. *Inorg. Chem.* **1994**, *33*, 3863.
 (10) Wang, P.; Humphry-Baker, R.; Moser, J. E.; Zakeeruddin, S. M.; Grätzel, M. *Chem. Mater.* **2004**, *16*, 3246.
 (11) Jin, Z.; Masuda, H.; Yamanaka, N.; Minami, M.; Nakamura, T.; Nishikitani, Y. *Chem. Lett.* **2009**, *38*, 44.

Emission spectra were recorded on a Spex Fluorolog 112 using a 90 ° optical geometry. The emitted light was detected with a Hamamatsu R928 photomultiplier operated in single-photon counting mode. Photoelectrochemical data were measured using a 1000 W xenon light source (Oriel, 91193) that was focused to give 1000 W/m², the equivalent of one sun at Air Mass (AM) 1.5, at the surface of the test cell. The light intensity was adjusted with a Si solar cell that was doubled-checked with an NREL-calibrated Si solar cell (PV Measurement Inc.). The applied potential and measured cell current were measured using a Keithley model 2400 digital source meter. The current-voltage characteristics of the cell under these conditions were determined by biasing the cell externally and measuring the generated photocurrent. This process was fully automated using Wavemetrics software.

Fluorine-doped tin oxide (FTO) glass plates (Pilkington TEC Glass-TEC 8, Solar 2.3 mm thickness) were cleaned in a detergent solution using an ultrasonic bath for 30 min and then rinsed with water and ethanol. Then, the plates were immersed in 40 mM TiCl₄ (aqueous) at 70 °C for 30 min and washed with water and ethanol. A transparent nanocrystalline layer was prepared on the FTO glass plates by using a doctor blade printing TiO₂ paste (Solaronix, Ti-Nanoxide T/SP), which was then dried for 2 h at 25 °C. The TiO₂ electrodes were gradually heated under an air flow at 325 °C for 5 min, at 375 °C for 5 min, at 450 °C for 15 min, and at 500 °C for 15 min. The thickness of the transparent layer was measured by using an Alpha-step 250 surface profilometer (Tencor Instruments, San Jose, CA). A paste containing 400 nm sized anatase particles (CCIC, PST-400C) was deposited by means of doctor blade printing to obtain the scattering layer and then dried for 2 h at 25 °C. The TiO₂ electrodes were gradually heated under an air flow at 325 °C for 5 min, at 375 °C for 5 min, at 450 °C for 15 min, and at 500 °C for 15 min. The resulting film was composed of a 10 μm thick transparent layer and a 4 μm thick scattering layer. The TiO₂ electrodes were treated again with TiCl₄ at 70 °C for 30 min and sintered at 500 °C for 30 min. Then, they were immersed in **JK-85** and **JK-86** (0.3 mM in EtOH and 10 mM CDCA) solutions and kept at room temperature for 24 h. FTO plates for the counter electrodes were cleaned in an ultrasonic bath in H₂O, acetone, and 0.1 M aqueous HCl, subsequently. The counter electrodes were prepared by placing a drop of an H₂PtCl₆ solution (2 mg of Pt in 1 mL of ethanol) on an FTO plate and heating it (at 400 °C) for 15 min. The dye adsorbed TiO₂ electrodes and the Pt counter electrodes were assembled into a

Scheme 1. Schematic Diagram for the Synthesis of Ruthenium Sensitizers JK-85 and JK-86^a

^a Reagents: (a) 2-(5-hexylthiophen-2-yl)-4,4,5,5-tetramethyl-1,3,2-dioxaborolane (**2a**) or 2-(2-hexylthieno[3,2-*b*]thiophen-5-yl)-4,4,5,5-tetramethyl-1,3,2-dioxaborolane (**2b**), Pd(PPh₃)₄/Na₂CO₃, THF/H₂O; (b) hexylamine, dppp, Pd₂(dba)₃, sodium *t*-butoxide, dry-toluene, 80 °C; (c) [Ru(Cl)₂(*p*-cymene)]₂, DMF, 70 °C; (d) bis(2,2'-bipyridyl)-4,4'-dicarboxylic acid, DMF, 160 °C; and (e) NH₄NCS, DMF, 140 °C.

sealed sandwich-type cell by heating at 80 °C using a hot-melt ionomer film (Surlyn) as a spacer between the electrodes. A drop of the electrolyte solution was placed in the drilled hole of the counter electrode and was driven into the cell via vacuum backfilling. Finally, the hole was sealed using additional Surlyn and a cover glass (0.1 mm thickness). Electron diffusion coefficients and lifetimes were measured by the stepped light-induced transient measurements of photocurrent and voltages (SLIM-PCV). The transients were induced by a stepwise change in the laser intensity. A diode laser ($\lambda = 635$ nm) as a continuous light source was modulated using a function generator (UDP-303, PNCYS Co. Ltd., Korea). The initial laser intensity was a constant 90 mW cm⁻² and was attenuated up to approximately 10 mW cm⁻² using a ND filter which was positioned at the front side of the fabricated samples (0.04 cm²). For the SLIM-PCV measurements, the TiO₂ thickness was controlled at approximately 8 μ m. The photocurrent and photovoltage transients were monitored using a digital oscilloscope through an amplifier. A total of five points were measured to determine the electron diffusion and lifetimes.

2-Bromo-4-(5-hexylthiophen-2-yl)pyridine (4a). 2-Bromo-4-iodopyridine **3** (651 mg, 2.3 mmol) and 2-(5-hexylthiophen-2-yl)-4,4,5,5-tetramethyl-1,3,2-dioxaborolane (677 mg, 2.3 mmol), Pd(PPh₃)₄ (133 mg, 5 mol %), and Na₂CO₃ (244 mg, 2.3 mmol) were dissolved in tetrahydrofuran (30 mL)/H₂O (20 mL) and the mixture was refluxed for 15 h. After evaporating the solvent under reduced pressure, H₂O (50 mL), and methylene chloride (50 mL) were added. The organic layer was separated and dried in MgSO₄. The solvent was removed under reduced pressure. The pure product **4a** was obtained by column chromatography on silica gel (CH₂Cl₂: hexane = 1:1, *R_f* = 0.41). Yield: 70%. ¹H NMR (CDCl₃): 8.25 (d, 1H, *J* = 5.1 Hz), 7.58 (s, 1H), 7.34–7.30 (m, 2H), 6.79 (d, 1H, *J* = 3.9 Hz), 2.82 (t, 2H, *J* = 7.4 Hz), 1.66 (qu, 2H, *J* = 7.4 Hz), 1.32 (m, 6H), 0.89 (t, 3H, *J* = 6.6 Hz). ¹³C NMR (CDCl₃): 150.5, 148.3, 147.8, 140.7, 139.1, 125.8, 124.3,

123.3, 117.8, 31.8, 31.6, 30.4, 28.5, 22.8, 14.5. Anal. Calcd for C₁₅H₁₈BrNS: C, 55.56; H, 5.59. Found: C, 56.76; H, 5.43.

2-Bromo-4-(2-hexylthieno[3,2-*b*]thiophen-5-yl)pyridine (4b). 2-Bromo-4-iodopyridine **3** (405 mg, 1.43 mmol), 2-(2-hexylthieno[3,2-*b*]thiophen-5-yl)-4,4,5,5-tetramethyl-1,3,2-dioxaborolane (500 mg, 1.43 mmol), Pd(PPh₃)₄ (83 mg, 5 mol %), and Na₂CO₃ (152 mg, 2.3 mmol) were dissolved in tetrahydrofuran (30 mL)/H₂O (20 mL), and the mixture was refluxed for 10 h. After evaporating the solvent under reduced pressure, H₂O (50 mL) and methylene chloride (50 mL) were added. The organic layer was separated and dried in MgSO₄. The solvent was removed under reduced pressure. The pure product **4b** was obtained by column chromatography on silica gel (ethyl acetate: hexane = 1:10, *R_f* = 0.24). Yield: 62%. ¹H NMR (CDCl₃): 8.27 (d, 1H, *J* = 5.1 Hz), 7.60 (s, 1H), 7.55 (s, 1H), 7.34 (d, 1H, *J* = 3.6 Hz), 6.93 (s, 1H), 2.87 (t, 2H, *J* = 7.1 Hz), 1.70 (m, 2H), 1.32 (m, 6H), 0.89 (t, 3H, *J* = 6.8 Hz). ¹³C NMR (CDCl₃): 151.8, 150.2, 149.0, 141.9, 141.0, 139.9, 138.3, 117.1, 116.2, 115.5, 113.4, 32.3, 31.0, 28.8, 26.9, 22.9, 14.2. Anal. Calcd for C₁₇H₁₈BrNS₂: C, 53.68; H, 4.77. Found: C, 53.66; H, 4.83.

***N*-Hexyl-4,4'-di(5-hexylthiophen-2-yl)-2,2'-dipyridylamine (5a).** 2-Bromo-4-(5-hexylthiophen-2-yl)pyridine (550 mg, 1.7 mmol) **4a**, hexylamine (0.1 mL, 0.8 mmol), 1,3-bis(diphenylphosphanyl)propane (27 mg, 0.07 mmol), dipalladiumtris(benzylideneacetone) (30 mg, 0.033 mmol), and sodium *tert*-butoxide (220 mg, 2.3 mmol) were combined in a Schlenk vessel under N₂. Dry toluene (50 mL) was then added and the resulting mixture stirred at 80 °C for 24 h. After evaporating the solvent under reduced pressure, H₂O (50 mL) and methylene chloride (50 mL) were added. The organic layer was separated and dried in MgSO₄. The solvent was removed under reduced pressure. The pure product **5a** was obtained by column chromatography on silica gel (ethyl acetate: hexane = 1:5, *R_f* = 0.42). Yield: 52%. ¹H NMR (CDCl₃): 8.31 (d, 2H, *J* = 5.7 Hz), 7.30 (s, 2H), 7.23 (d, 2H, *J* = 3.9 Hz), 7.02 (d, 2H, *J* = 5.7 Hz), 6.74 (d, 2H, *J* = 3.0 Hz), 4.24

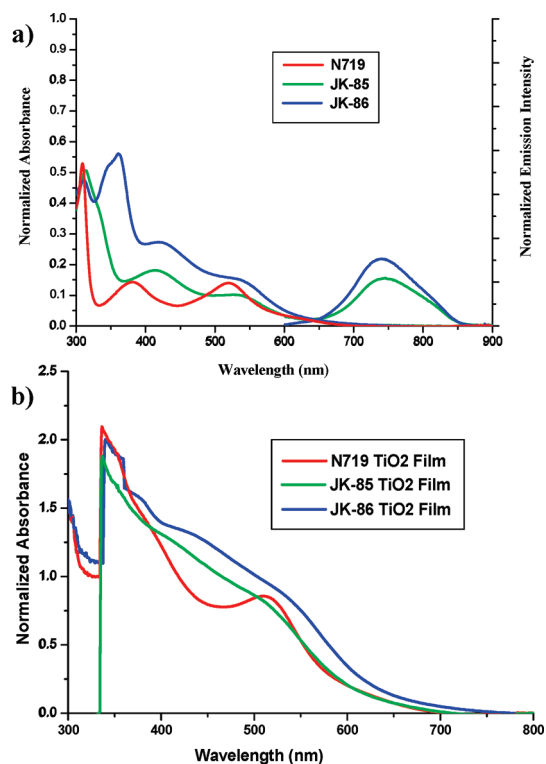


Figure 2. Absorption and emission spectra (a) of **JK-85** (green line), **JK-86** (blue line), and **N719** (red line) in ethanol and absorption spectra (b) of **JK-85** (green line), **JK-86** (blue line), and **N719** (red line) absorbed on TiO₂ film.

(t, 2H, $J = 7.5$ Hz), 2.80 (t, 4H, $J = 7.7$ Hz), 1.69 (m, 6H), 1.32 (m, 18H), 0.89 (m, 9H). ¹³C NMR (CDCl₃): 158.3, 148.9, 148.0, 143.0, 139.0, 125.4, 124.9, 113.5, 110.4, 48.6, 31.8, 31.6, 31.5, 30.4, 28.8, 28.5, 26.8, 22.8, 22.6, 14.1. Anal. Calcd for C₃₆H₄₉N₃S₂: C, 73.54; H, 8.40. Found: C, 73.36; H, 8.33.

N-Hexyl-4,4'-di(5-hexylthieno(3,2-*b*)thiophene)-2,2'-dipyridylamine (5b). The product **5b** was prepared using the same procedure of **5a** except that **4b** was used instead of **4a**. Yield: 56%. ¹H NMR (CDCl₃): 8.34 (d, 2H, $J = 4.8$ Hz), 7.51 (s, 2H), 7.36 (s, 2H), 7.07 (d, 2H, $J = 3.9$ Hz), 6.90 (s, 2H), 4.25 (t, 2H, $J = 6.6$ Hz), 2.86 (t, 4H, $J = 6.8$ Hz), 1.72 (m, 6H), 1.33 (m, 18H), 0.90 (m, 6H). ¹³C NMR (CDCl₃): 158.3, 150.2, 149.0, 143.3, 141.5, 139.4, 138.1, 117.5, 116.5, 113.5, 110.4, 48.07, 31.8, 31.6, 31.5, 31.3, 28.8, 28.5, 26.9, 22.8, 22.7, 14.2. Anal. Calcd for C₄₀H₄₉N₃S₄: C, 68.62; H, 7.05. Found: C, 66.85; H, 7.13.

cis-Bis(thiocyanato)-(2,2'-bipyridyl-4,4'-dicarboxylato)[{*N*-hexyl-4,4'-di(5-hexylthiophen-2-yl)-2,2'-dipyridylamine}ruthenium(II) **JK-85.** A mixture *N*-hexyl-4,4'-di(5-hexylthiophen-2-yl)-2,2'-dipyridylamine (90 mg, 0.153 mmol) and a dichloro(*p*-cymene)-ruthenium(II) dimer (46 mg, 0.077 mmol) in argon-degassed DMF (15 mL) was stirred at 70 °C for 4 h under reduced light. Subsequently, 4,4'-dicarboxylic-2,2'-bipyridine (37 mg, 0.153 mmol) was added into the flask, and the reaction mixture was stirred at 160 °C for 4 h. An excess of NH₄NCS (116 mg, 1.53 mmol) was added to the resulting dark solution, and the reaction continued for another 4 h at 140 °C. Then the reaction mixture was cooled to room temperature, and the solvent was removed under vacuum. Water was added to induce the precipitate. The resulting solid was filtered and washed with water and dried under vacuum. The resulting solid was dissolved in methanol containing 2.2 equiv of tetrabutylammonium hydroxide to confer solubility by deprotonating the carboxylic group and purified on a Sephadex LH-20 column with methanol

as eluent. The collected main band was concentrated, and the solution pH was lowered to 5.1 using 0.02 M nitric acid. The precipitate was collected on a sintered glass crucible by suction filtration and dried in air. Yield: 30%. ¹H NMR (CD₃OD): 9.56 (d, 1H), 8.96 (d, 1H), 8.85 (s, 1H), 8.78 (s, 1H), 8.29 (d, 1H), 8.16 (d, 1H), 7.74 (m, 3H), 7.53 (m, 2H), 7.42 (d, 1H), 7.15 (s, 1H), 6.94 (m, 2H), 6.80 (d, 1H), 4.21 (t, 1H), 3.78 (t, 1H), 2.90 (t, 2H), 2.79 (t, 2H), 1.64 (m, 6H), 1.36 (m, 18H), 0.86 (m, 9H). Anal. Calcd for C₅₀H₅₇N₇O₄RuS₄: C, 57.23; H, 5.48. Found: C, 56.95; H, 5.63.

cis-Bis(thiocyanato)-(2,2'-bipyridyl-4,4'-dicarboxylato)[{4,4'-di(5-hexylthieno(3,2-*b*)thiophene)-2,2'-dipyridylamine}ruthenium(II) **JK-86.** The product **JK-86** was prepared using the same procedure of **JK-85** except that **5b** was used instead of **5a**. Yield: 27%. ¹H NMR (CD₃OD): 9.56 (d, 1H), 8.97 (d, 1H), 8.85 (s, 1H), 8.78 (s, 1H), 8.28 (d, 1H), 8.16 (d, 1H), 8.05 (s, 1H), 7.76 (m, 3H), 7.60 (s, 1H), 7.38 (d, 1H), 7.21 (d, 1H), 7.06 (s, 1H), 6.96 (s, 1H), 6.88 (d, 1H), 4.26 (t, 1H), 3.80 (t, 1H), 2.81 (m, 4H), 1.60 (m, 6H), 1.34–1.21 (m, 18H), 0.81 (m, 9H). Anal. Calcd for C₅₄H₅₇N₇O₄RuS₆: C, 55.84; H, 4.95. Found: C, 55.93; H, 4.78.

Results and Discussion

The novel ruthenium sensitizers **JK-85** and **JK-86** were prepared by the stepwise synthetic protocol illustrated in Scheme 1. New sensitizers are readily synthesized in five steps starting from the 2-bromo-4-iodopyridine. The Suzuki coupling reaction¹² of **1** with 2-(5-hexylthiophen-2-yl)-4,4,5,5-tetramethyl-1,3,2-dioxaborolane **2a** or 2-(2-hexylthieno[3,2-*b*]thiophen-5-yl)-4,4,5,5-tetramethyl-1,3,2-dioxaborolane **2b** yielded **3a–3b**. Conjugated dipyridylamine ligands **4a–4b** were prepared by the Ullman coupling reaction¹³ of **3a–3b** with hexylamine. **JK-85** and **JK-86** were obtained in one pot synthesis from the sequential reaction of [Ru(*p*-cymene)Cl₂]₂ with **4a–4b** followed by the reaction of the resulting mononuclear complex with 4,4'-dicarboxy-2,2'-bipyridine. The chloro complexes reacted with an excess of ammonium thiocyanate ligand to afford the ruthenium dyes **JK-85** and **JK-86**. The analytical and the spectroscopic data of both dyes are consistent with the formulated structures.

Figure 2a shows the UV–vis spectra of **JK-85** and **JK-86** in EtOH, in addition to the **N719** absorption spectrum as a reference. The data are collected in Table 1. The strong absorption band of **JK-86** at 358 nm is due to a bipyridine intraligand $\pi-\pi^*$ transition. Two absorption bands of **JK-86** at 422 and 543 nm are the characteristic metal-to-ligand charge transfer bands (MLCT). In EtOH, the low energy MLCT band of **JK-86** at 547 nm is 4 and 26 nm red-shifted relative to that of **N719** and **JK-85**, respectively. The red-shifted band is attributable to the increase of the π -conjugation system in an ancillary ligand. The threshold wavelengths of absorption spectra for **JK-85** and **JK-86** are 700 and 760 nm, respectively, indicating that the introduction of a thiophene or

- (12) (a) Hoffmann, K. J.; Bakken, E.; Samuelsen, E. J.; Carlsen, P. H. *J. Synth. Met.* **2000**, *113*, 39. (b) Huang, C.-H.; McClenaghan, N. D.; Kuhn, A.; Hofstraat, J. W.; Bassan, D. M. *Org. Lett.* **2005**, *7*, 3409. (c) Turbiez, M.; Frère, P.; Allain, M.; Vidélot, C.; Ackermann, J.; Roncali, J. *Chem.—Eur. J.* **2005**, *11*, 3742.
- (13) Bushby, R. J.; McGill, D. R.; Ng, K. M.; Taylor, N. *J. Mater. Chem.* **1997**, *7*, 2343.

Table 1. Optical, Oxidation, and DSSC Performance Parameters of Dyes

dye	$\lambda_{\text{abs}},^a$ nm ($\epsilon, \text{M}^{-1} \text{cm}^{-1}$)	$E_{\text{ox}},^b$ V	$E_{0-0},^c$ V	$E_{\text{LUMO}},^d$ V	$J_{\text{sc}},$ mA cm^{-2}	$V_{\text{oc}},$ V	FF	$\eta,^e$ %
JK-85	527 (10 220); 412 (18 130)	1.03	1.94	-0.91	16.50	0.71	0.65	7.66
JK-86	525 (15 580); 418 (27 340)	1.02	1.91	-0.89	18.32	0.68	0.72	9.03
N719	521 (13 970); 380 (14 268)				16.15	0.74	0.74	8.88

^a Absorption spectra were measured in ethanol solution. ^b Oxidation potential of dyes on TiO₂ were measured in CH₃CN with 0.1 M (*n*-C₄H₉)₄NPF₆ with a scan rate of 50 mV s⁻¹ (vs NHE). ^c E_{0-0} was determined from the intersection of absorption and emission spectra in ethanol. ^d E_{LUMO} was calculated by $E_{\text{ox}} - E_{0-0}$. ^e Performances of DSSCs were measured with a 0.18 cm² working area. Electrolyte: 0.6 M DMPImI, 0.05 M I₂, 0.1 M LiI, and *tert*-butylpyridine in acetonitrile.

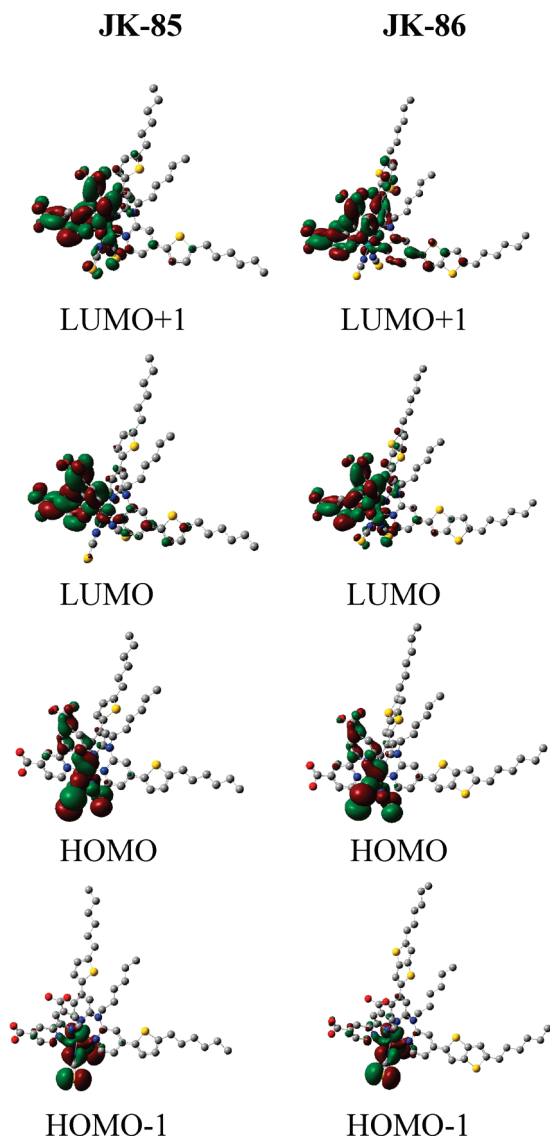


Figure 3. Isodensity surface plots of the HOMO, HOMO-1, LUMO, and LUMO+1 of JK-85 and JK-86.

thienothiophene unit into the pyridyl ligand expanded the conjugation resulting in a wide absorption in the red visible region. The molar extinction coefficient of the lower energy MLCT band for JK-86 ($\epsilon = 15\,580 \text{ M}^{-1} \text{cm}^{-1}$) is higher than those of N719 ($\epsilon = 13\,970 \text{ M}^{-1} \text{cm}^{-1}$) and JK-85 ($\epsilon = 10\,220 \text{ M}^{-1} \text{cm}^{-1}$). The absorption spectra of JK-85 and JK-86 on TiO₂ film are broadened due to the interaction of the anchoring group with the surface titanium ion, ensuring a good light-harvesting efficiency (Figure 2b). The enhanced red absorption of JK-86 render it an attractive candidate as a panchromatic

charge-transfer sensitizer for DSSCs. Strong luminescence maxima around 745 nm of JK-85 and JK-86 were obtained by exciting within the MLCT absorption band at 298 K in an air-equilibrated ethanol solution.

To evaluate the possibility of electron transfer from the excited state of the dye to the conduction band of TiO₂ electrode, we perform cyclic voltammetry measurements on JK-85 and JK-86 in CH₃CN with TBAPF₆ as the supporting electrolyte. The two ruthenium dyes on TiO₂ show quasi-reversible couples. The oxidation potentials of JK-85 and JK-86 were measured to be 1.03 and 1.02 V versus NHE, respectively, whereas that of N719 is reported to be 0.85 V versus NHE.¹⁴ The uphill energy offset of the HOMO in both dyes relative to that (+0.5 V) of the triiodide/iodide couple could lead to fast dye regeneration. The reduction potentials of JK-85 and JK-86 calculated from the oxidation potential and the E_{0-0} determined from the intersection of absorption and emission spectra are listed in Table 1. The excited-state oxidation potential is calculated to be -0.91 V for JK-85 and -0.89 V for JK-86 versus NHE. The downhill energy offset of the LUMO in both dyes compared to the conduction band level of TiO₂ at approximately -0.5 V versus NHE ensures an enough driving force for charge generation.¹⁵

To gain insight into the geometrical electronic structure of the two dyes we performed DFT calculations on the JK-85 and JK-86 using density functional theory. Structures were optimized using the Vienna ab initio simulation package (VASP).¹⁶ Projected augmented waves¹⁷ (PAW) were employed to describe the electron-ion interaction, and the local density approximation (LDA) was adopted for the exchange correlation functional. For optimized structures, we find that electronic structures calculated using the LDA within the PAW agree well with those from separate Gaussian03 calculations using the Lanl2dz basis set. The first two HOMOs exhibit ruthenium t_{2g} character in addition to a significant contribution from the thiocyanate ligand (Figure 3). The HOMO of JK-86 is a combination of π -bonding orbital of the dcby and big contribution from the NCS ligand and the

(14) Nazeeruddin, M. K.; Kay, A.; Rodicio, I.; Humphry-Baker, R.; Muller, E.; Liska, P.; Vlachopoulos, N.; Grätzel, M. *J. Am. Chem. Soc.* **1993**, *115*, 6382.

(15) (a) Bond, A. M.; Deacon, G. B.; Howitt, J.; MacFarlane, D. R.; Spiccia, L.; Wolfbauer, G. *J. Electrochem. Soc.* **1999**, *146*, 648. (b) Wang, P.; Zakeeruddin, S. M.; Moser, J.-E.; Grätzel, M. *J. Phys. Chem. B* **2003**, *107*, 13280.

(16) (a) Kresse, G.; Hafner, J. *Phys. Rev. B* **1993**, *47*, RC558. (b) Kresse, G.; Furthmüller, J. *Phys. Rev. B* **1996**, *54*, 11169.

(17) Kresse, G.; Joubert, D. *Phys. Rev. B* **1999**, *59*, 1758.

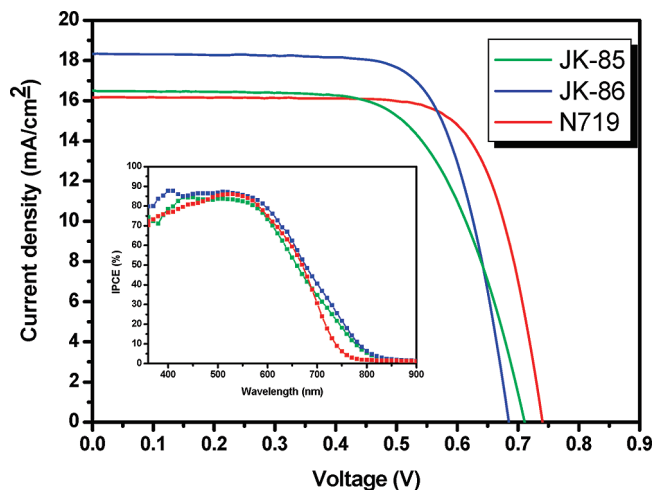


Figure 4. J - V curves and IPCE of **JK-85** (green line), **JK-86** (blue line), and **N719** (red line).

ruthenium center. The LUMO and LUMO+1 of **JK-86** are π^* orbitals delocalized on the dc bpy ligands. Examination of the HOMO and LUMO of two sensitizers indicates that HOMO–LUMO excitation moved the electron distribution from the NCS unit to the 4,4'-dicarboxy-2,2'-bipyridine, and the photoinduced electron transfer from the dye to TiO_2 electrode can be efficiently mediated by the HOMO–LUMO transition.

The photocurrent action spectra of the three sensitizer are presented in the inset of Figure 4. The incident-photon-to-current conversion efficiency (IPCE) of **JK-86** exceeds 80% in a broad spectral range from 420 to 610 nm, reaching its maximum of 85% at 540 nm. The IPCE tails off toward 830 nm, contributing to the broad spectral light harvesting that is characteristic of pyridyl ruthenium dyes. The **JK-85** and **JK-86** sensitizers' IPCE spectra are more enhanced in the red region compared to that of **N719** as a result of extended π -conjugation, which is consistent with the absorption spectra of the **JK-85** and **JK-86** sensitizers. From the overlap integral of this curve (IPCE) of **JK-86** with the standard global AM 1.5 solar emission spectrum, a short-circuit photocurrent density of 17.75 mA cm^{-2} is calculated, which is in good agreement with the measured device photocurrent. The J - V curve for the DSSCs based on **JK-85** and **JK-86** is presented and compared with that of the **N719** dye in Figure 4. Photovoltaic performance of the **JK-85** and **JK-86** sensitized cells with an active cell area of 0.18 cm^2 using a black tape mask under simulated AM 1.5 solar condition is summarized in Table 1. The **JK-85** and **JK-86** sensitized cell gave short circuit photocurrent densities (J_{sc}) of 16.50 and 18.32 mA cm^{-2} , open circuit voltages (V_{oc}) of 0.71 and 0.68 V , and fill factors of 0.65 and 0.72 , corresponding to overall conversion efficiencies (η) of 7.66 and 9.03% , respectively. Under the same condition, the **N719** sensitized cell gave a J_{sc} of 16.15 mA cm^{-2} , a V_{oc} of 0.74 V , and a fill factor of 0.74 , corresponding to η of 8.88% . The J_{sc} enhancement of **JK-86** relative to **N719** can be related to the expansion of the π -conjugated system of **JK-86**. A slightly lower V_{oc} of **JK-86** compared

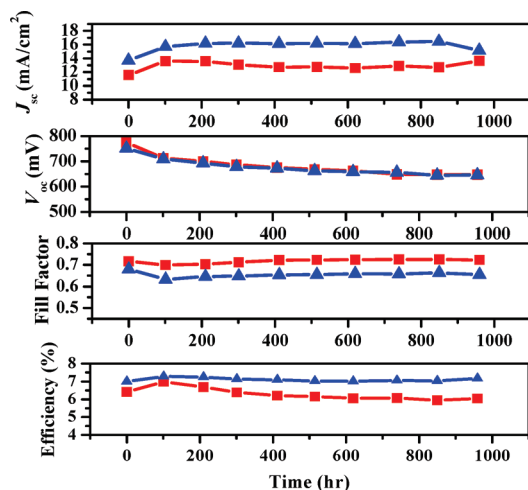


Figure 5. Evolution of solar cell parameters with **JK-85** (red line) and **JK-86** (blue line) during visible-light soaking (AM 1.5G, 100 mW/cm^2) at 60°C . A 420 nm cutoff filter was put on the cell surface during illumination. Electrolyte: DMPPI (0.6 M), I_2 (0.1 M), NMBI (0.5 M), and PVDF-HFP ($5 \text{ wt } \%$) in MPN.

to those of **JK-85** and **N719** can be correlated with the increase of dark current due to the decreased amount of dye adsorbed on TiO_2 . To clarify the above results, we measured the amount of dyes adsorbed on TiO_2 film by desorbing the dyes from the TiO_2 surface with KOH. The adsorbed amounts of $4.62 \times 10^{-7} \text{ mmol cm}^{-2}$ for **JK-85**, $3.76 \times 10^{-7} \text{ mmol cm}^{-2}$ for **JK-86**, and $5.84 \times 10^{-7} \text{ mmol cm}^{-2}$ for **N719** are observed. The low adsorption of **JK-86** can be due to the presence of two bulky organic units and low solubility. It is believed that the electron recombination occurred more significantly in the photoelectrodes adsorbing the dyes with more bulky structure owing to the relatively large TiO_2 surface area unoccupied by dye molecules.

Since the long-term stability is very critical for sustained cell operation, we replaced a volatile liquid electrolyte with a quasi-solid-state electrolyte. Figure 5 shows the photovoltaic performance during long-term light soaking and thermal stability tests of **JK-85** and **JK-86** using a quasi-solid-state electrolyte composed of 0.1 M I_2 , 0.5 M NMBI (*n*-methyl-benzimidazole), 0.6 M DMPPI (1-propyl-2,3-dimethylimidazolium iodide), and $5 \text{ wt } \%$ PVDF-HFP (poly(vinylidene fluoride-*co*-hexafluoropropylene)) in MPN (3-methoxypropionitrile). The device of **JK-86** showed an excellent long-term stability and a high conversion efficiency of 7.00% . After 1000 h of light soaking at 60°C , the photovoltaic performance of 7.02% revealed almost no change compared to the initial value (7.00%). After 1000 h of light soaking, the V_{oc} of **JK-86** decreased by 106 mV , but the loss was compensated by an increase in the short-circuit current density. The long-term stability of the device is remarkable because only a few ruthenium polypyridyl sensitizers passed the light-soaking stress for 1000 h while retaining an efficiency over 6.5% using a quasi-solid electrolyte.¹⁸

(18) Wang, P.; Zakeeruddin, S. M.; Moser, J. E.; Nazeeruddin, M. K.; Sekiguchi, T.; Grätzel, M. *Nat. Mater.* **2003**, *2*, 402.

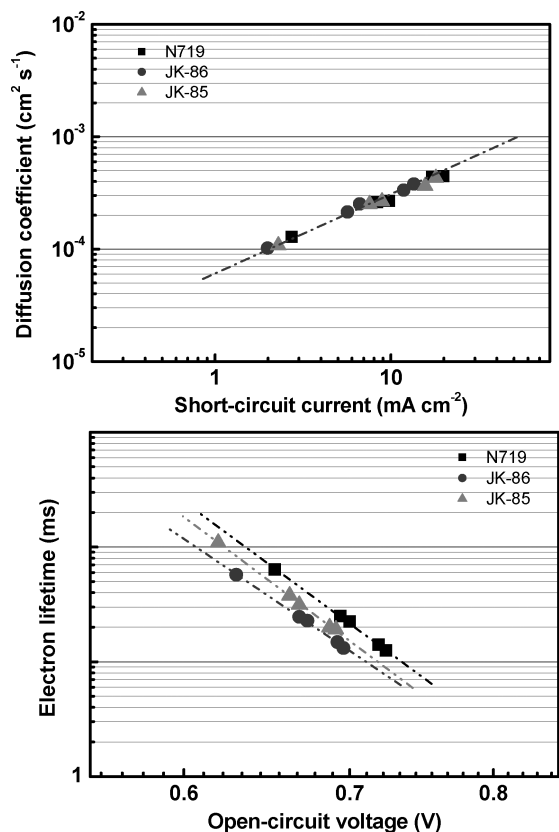


Figure 6. Electron diffusion coefficients (a) and electron lifetimes (b) in the photoelectrodes adsorbing different dyes (i.e., JK-85, JK-86, and N719).

The robust and high efficiency cells were further tested for long-term stability using a quasi-solid electrolyte at 85 °C. The device employing JK-86 also showed an excellent long-term stability. The initial efficiency of 6.82% slightly decreased to 6.60% following the 1000 h accelerated test at 85 °C (Supporting Information, Figure S). During this aging process, the V_{oc} decreased by 71 mV. The drop in V_{oc} was compensated by an increase in J_{sc} . The enhanced long stability of JK-86 can be attributed to the substituted hexyl group by preventing the approach of acceptors to the TiO_2 surface, resulting in preventing the dark current.¹⁹

Figure 6 shows the electron diffusion coefficients (D_e) and lifetimes (τ_e) of the DSSCs employing different dyes (i.e., JK-85, JK-86, and N719) displayed as a function of the J_{sc} .

The D_e values of the photoanodes adsorbing the two ruthenium dyes JK-85 and JK-86 are shown to be very similar to that of N719 at the identical short-circuit current conditions. This result means that the D_e values are hardly affected by structural changes in the dye molecules. On the other hand, the significant difference in the τ_e values was observed among the cells employing different dyes. The different τ_e values might be caused by the different molecular size and structures of the dyes. The τ_e values of JK-86 were slightly smaller than those of

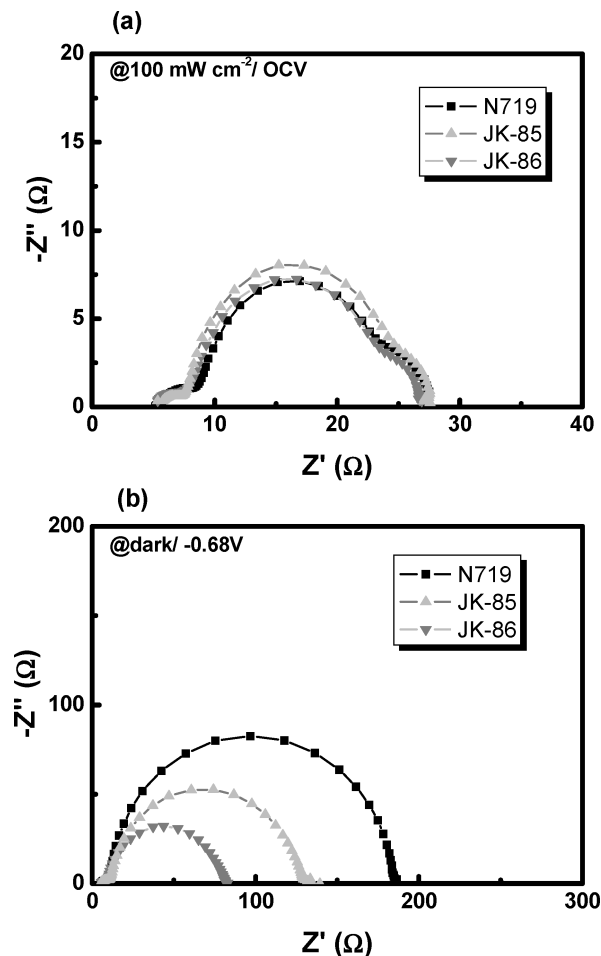


Figure 7. Electrochemical impedance spectra measured under the illumination (100 mW cm^{-2}) and at the dark for the cells employing different dyes (i.e., JK-85, JK-86, and N719).

JK-85 and N719, demonstrating the decreased amount of dyes on TiO_2 due to the steric hindrance caused by the bulky configuration. The electron recombination rates were dependent upon the molecular structures and the intermolecular π - π stacking interactions of the dyes due to the different coverage on the TiO_2 surface. The results of the electron lifetimes are well consistent with those of the V_{oc} shown in Table 1.

Figure 7 shows the ac impedance spectra measured under (a) illumination and (b) dark conditions. Under open-circuit conditions and illumination of 100 mW cm^{-2} , the radius of the intermediate frequency semicircle in the Nyquist plot decreased in the order of JK-85 (16.36Ω) > JK-86 (14.8Ω) \approx N719 (14.1Ω), indicating the improved charge generation and transport. The result is in good accord with that of the short-circuit current trend shown in Table 1. In the dark under forward bias (-0.67 V), the semicircle in the intermediate frequency regime demonstrates the dark reaction impedance caused by the electron transport from the conduction band of TiO_2 to I_3^- ions in electrolyte. The increased radius of the semicircle in the intermediate frequency regime implies a reduced electron recombination rate at the dyed $\text{TiO}_2/\text{electrolyte}$ interface. In dark, the radius of the intermediate-frequency semicircle showed the increasing order of

(19) (a) Kroeze, J. E.; Hirata, N.; Koops, S.; Nazeeruddin, M. K.; Schmidt-Mende, L.; Grätzel, M.; Durrant, J. R. *J. Am. Chem. Soc.* **2006**, *128*, 16377. (b) Koumura, N.; Wang, Z.-S.; Mori, S.; Miyashita, M.; Suzuki, E.; Hara, K. *J. Am. Chem. Soc.* **2006**, *128*, 14256.

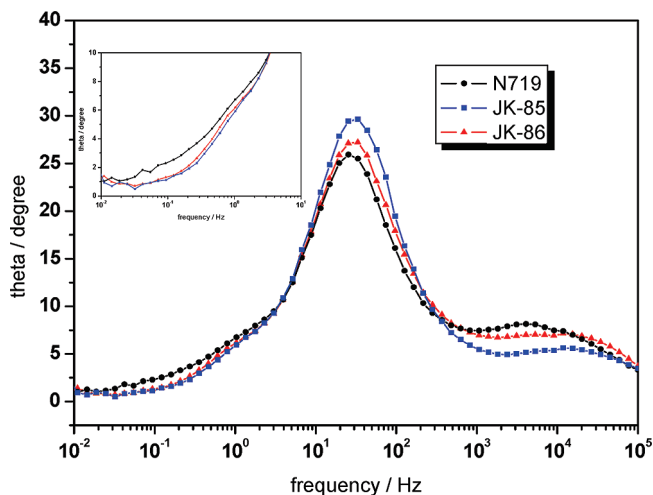


Figure 8. Impedance spectra of DSCs based on **N719**, **JK-85**, and **JK-86** measured at OCV bias under illumination. Inset: Bode phase plot at low-frequency.

N719 (168.1Ω) > **JK-85** (116.4Ω) > **JK-86** (63.35Ω), in accord with the trends of V_{oc} and τ_e values.

The Bode phase plots in Figure 8 illustrate the dye structure-device function in terms of the interfacial charge transfer processes. The low-frequency peaks observed in the Bode plots correspond to triiodide diffusion in the electrolyte. The low-frequency maximum of **JK-85** and **JK-86** is slightly higher than that of **N719**. Therefore the triiodide diffusion in the porous network is apparently enhanced in the **JK-85** and **JK-86** sensitizers relative to **N719**. It may be interpreted that aggregate formation on

TiO_2 films by **N719** impairs the transport of the triiodide ions in the pores of the TiO_2 film, resulting in increasing the diffusion impedance.

In conclusion, we designed and synthesized two efficient ruthenium sensitizers containing a highly conjugated di-pyridylamine derivatives. A solar-cell device based on the sensitizer **JK-86** in conjunction with a volatile electrolyte yielded an overall conversion efficiency of 9.03%, whereas the conversion efficiency of a device of **JK-86** using a polymer gel electrolyte gave an higher efficiency of 7.00%. Moreover, the **JK-86** device showed an excellent stability under light soaking at 60 °C for 1000 h. The high efficiency and excellent stability may be attributed to the introduction of two hydrophobic alkyl chains and extend conjugation on the bipyridyl ligand. We believe that the development of highly efficient DSSC devices with robustness is possible through the structural modifications, and work on these is now in progress.

Acknowledgment. We are grateful to the KOSEF through the National Research Laboratory (No. R0A-2005-000-10034-0) program, WCU program (No. R31-2008-000-10035-0), and the Ministry of Information & Communication, Korea, under ITRC (No. ITRC 2008 C 1090 0904 0013) and BK21. Computations were performed using a Super-computer of the Korea Institute of Science and Technology Information under Grant KSC-2008-S03-0008.

Supporting Information Available: Long-term stability test at 85 °C (PDF). This information is available free of charge via the Internet at <http://pubs.acs.org>.